UNIVERSITY OF BIRMINGHAM
University of Birmingham Research at Birmingham

Petrogenesis of plagiogranites in the Muslim Bagh Ophiolite, Pakistan

Cox, Daniel; Kerr, Andrew; Hastie, Alan; Kakarc, Ishaq

DOI:
10.1017/S0016756818000250

License:
None: All rights reserved

Document Version
Peer reviewed version

Citation for published version (Harvard):
Cox, D, Kerr, A, Hastie, A & Kakarc, I 2018, 'Petrogenesis of plagiogranites in the Muslim Bagh Ophiolite, Pakistan: implications for the generation of Archean continental crust', *Geological Magazine*, vol. 156, no. 5, pp. 874-888. https://doi.org/10.1017/S0016756818000250

Link to publication on Research at Birmingham portal

Publisher Rights Statement:
Published in Geological Magazine on 02/04/2018

DOI: 10.1017/S0016756818000250

COPYRIGHT: © Cambridge University Press 2017

General rights
Unless a licence is specified above, all rights (including copyright and moral rights) in this document are retained by the authors and/or the copyright holders. The express permission of the copyright holder must be obtained for any use of this material other than for purposes permitted by law.

•Users may freely distribute the URL that is used to identify this publication.
•Users may download and/or print one copy of the publication from the University of Birmingham research portal for the purpose of private study or non-commercial research.
•User may use extracts from the document in line with the concept of ‘fair dealing’ under the Copyright, Designs and Patents Act 1988 (?)
•Users may not further distribute the material nor use it for the purposes of commercial gain.

Where a licence is displayed above, please note the terms and conditions of the licence govern your use of this document.

When citing, please reference the published version.

Take down policy
While the University of Birmingham exercises care and attention in making items available there are rare occasions when an item has been uploaded in error or has been deemed to be commercially or otherwise sensitive.

If you believe that this is the case for this document, please contact UBIRA@lists.bham.ac.uk providing details and we will remove access to the work immediately and investigate.

Download date: 25. Apr. 2024

Petrogenesis of plagiogranites in the Muslim Bagh Ophiolite, Pakistan: implications for the generation of Archean continental crust

Category: original article

Daniel Cox[a,b*], Andrew C. Kerr[b], Alan R. Hastie[a], M. Ishaq Kakar[c]

[a] School of Geography, Earth and Environmental Sciences, University of Birmingham, Edgbaston, Birmingham, B15 2TT, U.K.

[b] School of Earth and Ocean Sciences, Cardiff University, Main Building, Park Place, Cardiff, CF10 3AT, U.K.

[c] Centre of Excellence in Mineralogy, University of Balochistan, Quetta, Pakistan.

* Corresponding author. E-mail: DXC506@student.bham.ac.uk, School of Geography, Earth and Environmental Sciences, University of Birmingham, Edgbaston, Birmingham, B15 2TT, U.K.

Andrew C. Kerr: KerrA@cardiff.ac.uk; Alan R. Hastie: A.R.Hastie@bham.ac.uk; M. I. Kakar: kakarmi.cemuob@gmail.com.

Abstract

High-SiO_2 rocks referred to as oceanic plagiogranites are common within the crustal sequences of ophiolites; however, their mode of petrogenesis is controversial with both late-stage fractional crystallisation and partial melting models being proposed. Here, we present new whole rock data from plagiogranitic dyke-like bodies and lenses from the lower and middle sections of the sheeted dyke complex of the Cretaceous Muslim Bagh Ophiolite, north-western Pakistan. The plagiogranites have similar geochemical signatures that are inconsistent with them being the fractionation products of the mafic units of the Muslim Bagh Ophiolite. However, the plagiogranites all display very low TiO_2 contents (<0.4 wt. %), implying that they formed by partial melting of mafic rocks. Melt modelling of a crustal gabbro from the Muslim Bagh Ophiolite shows that the trace element signature of the plagiogranites can be replicated by 5 – 10% melting of a crustal hornblende gabbro, with amphibole as a residual phase, resulting in a concave-up middle rare earth element pattern. Compositional similarities between the Muslim Bagh Ophiolite plagiogranites and Archean TTG (trondhjemite – tonalite – granodiorite) has implications for the generation of juvenile Archean continental crust. As the Muslim Bagh Ophiolite was derived in a supra-subduction zone, it is suggested that some Archean TTG may have been derived from melting of mafic upper crust in early subduction-like settings. However, due to the small volume of Muslim Bagh Ophiolite plagiogranites, it is inferred that they can be instructive on the petrogenesis of some, but not all, of Archean TTG.

Keywords: Pakistan, Muslim Bagh, Ophiolite, Oceanic Plagiogranite, Partial Melting

1. Introduction

Within obducted Phanerozoic ophiolite sequences, suites of felsic rocks termed "oceanic plagiogranites" (Coleman & Peterman, 1975; Le Maitre et al., 2002, p. 118) occur as small volume (<10%) components (Coleman & Peterman, 1975; Koepke et al., 2007). The petrogenesis of these plagiogranites is controversial, having been variously proposed to have formed by the late-stage crystallisation of mafic melts (Coleman & Peterman, 1975), hydrous partial melting (and assimilation) of mafic rocks (Gerlach et al., 1981; Amri et al., 1996; Gillis & Coogan, 2002; France et al., 2009, 2010; Erdmann et al., 2015) or silicate–liquid immiscibility (Dixon & Rutherford, 1979).

Significantly, plagiogranites have compositional similarities to trondhjemite, tonalite and granodiorite (TTG) rocks that are common in Archean terranes from 4.0 – 2.5 Ga (e.g., Drummond et al., 1996; Kerrich & Polat, 2006; Moyen & Martin, 2012; Kusky et al., 2013). Although themselves controversial, Archean TTG are considered, by many, to be generated by the partial melting of mafic igneous source regions (e.g., Drummond et al., 1996; Foley et al., 2002; Rapp et al., 2003; Martin et al., 2005; Moyen & Stevens, 2006; Nutman et al., 2009; Hastie et al., 2015, 2016). Significantly, the compositional similarity of Phanerozoic oceanic plagiogranites to Archean TTG suggests that if we can better understand how plagiogranites are formed, it may further our understanding of how primitive continents were formed on the early Earth (Rollinson, 2008, 2009, 2014).

In this paper, we present major and trace element data for oceanic plagiogranites sampled from a sheeted dyke complex within the Late Cretaceous (Neo-Tethyan) Muslim Bagh Ophiolite in north-western Pakistan (Kakar et al., 2012). We investigate the composition of these plagiogranitic lenses and dykes in the sheeted dyke complex to determine their petrogenesis. We then discuss the implications of these results for the generation of Archean continental crust.

2. Ophiolites and plagiogranites

Oceanic plagiogranites are found throughout geological time, in both the Precambrian (e.g., Samson et al., 2004; Kaur & Mehta, 2005) and Phanerozoic (e.g., Tilton et al., 1981; Flagler & Spray, 1991; Rollinson, 2009), and are common in the crustal sections of ophiolitic sequences (e.g., Flagler & Spray, 1991; Amri et al., 1996; Twining, 1996; Yaliniz et al., 2000; Samson et al., 2004). Plagiogranites have also been recovered from recent oceanic ridge systems around the world, for example, the Southwest Indian (e.g., Dick et al., 2000), Central Indian (e.g., Nakamura et al., 2007) and Mid-Atlantic Ridges (e.g., Aranovich et al., 2010; Grimes et al., 2011). The morphology of oceanic plagiogranites is complex and they have been documented in a range of intrusive forms, from small veins (millimetre- to centimetre-scale; e.g., Dick et al., 2000; Nakamura et al., 2007), to dykes and inclusions (millimetre- to metre-scale; e.g., Flagler and Spray, 1991; Jafri et al., 1995), to large kilometre-scale plutonic bodies (e.g., Rollinson, 2009).

Oceanic plagiogranites are predominantly composed of sodic plagioclase and quartz, with mafic (usually hornblende and pyroxene) minerals being minor constituents (<10%), and K-feldspar being a rare phase. In addition to the major modal mineralogy, several accessory minerals including zircon, magnetite and ilmenite are also commonly found in oceanic plagiogranites (Coleman & Peterman, 1975; Coleman & Donato, 1979).

In the mid-1970s, plagiogranites were considered to represent the likely silicic end products of crystallising basaltic magmas (Coleman & Peterman, 1975; Coleman & Donato, 1979).

Although such a crystallisation model is still advocated by some authors, who have shown that oceanic plagiogranites fall along the liquid lines of descent of evolving magmas in other ophiolite units (e.g., Jafri et al., 1995; Rao et al., 2004; Freund et al., 2014), the genesis of oceanic plagiogranites is more commonly attributed to the partial melting of mafic igneous source regions (Gerlach et al., 1981; Flagler & Spray, 1991; see Koepke et al., 2007 for a review of oceanic plagiogranite petrogenesis models). Melting models propose that oceanic plagiogranites are derived through partial melting of mafic protoliths; either by hydrous partial melting of crustal gabbros (e.g., Gerlach et al., 1981; Flagler & Spray, 1991; Amri et al., 1996) or the assimilation and partial melting of hydrothermally altered sheeted dykes (e.g., Gillis & Coogan, 2002; France et al., 2009, 2010; Erdmann et al., 2015).

A partial melting origin is supported by the experimental work of Koepke et al. (2004), who undertook hydrous melting experiments on oceanic cumulate gabbros at temperatures from 900 – 1060 °C and a relatively shallow pressure of 0.2 GPa. Koepke et al. (2004) showed that lower temperature runs (900 – 940 ºC) generated partial melts with similar major element compositions to natural oceanic plagiogranites. One important finding from the P-T experiments was that the melts replicate the low TiO_2 concentrations that can be found in oceanic plagiogranites (<1 wt.%; Koepke et al., 2004). Low TiO_2 is now considered a key characteristic of oceanic plagiogranites that have been derived by partial melting, as opposed to oceanic plagiogranites derived through fractional crystallisation that display higher TiO_2 contents (>1 wt.%; Koepke et al., 2004, 2007). Further experimental work conducted by France et al. (2010) has also shown that oceanic plagiogranites derived by partial melting have low TiO2 contents, supporting the experimental work of Koepke et al. (2004).

3. Geological setting

3.a. Regional setting

The Muslim Bagh Ophiolite (MBO) is one of a number of ophiolites (i.e., Bela, Waziristan, Khost, Zhob) of Neo-Tethyan origin (Kakar et al., 2014) that comprise the Western Ophiolite Belt of the Zhob Valley, north-western Pakistan (Ahmad & Abbas, 1979; Mahmood et al., 1995; Gnos et al., 1997) (Fig. 1). These ophiolites represent fragments of Neo-Tethyan Ocean crust that were obducted onto the margin of the Indian continent prior to its final collision with Asia (e.g., Gnos et al., 1997; Khan et al., 2009) and, therefore, they mark the boundary between the Indian and Eurasian Plates (Asrarullah et al., 1979; Mengal et al., 1994; Gnos et al., 1997).

The Muslim Bagh area comprises four main geological units (Fig. 1). These units are (south to north) the Indian Passive Margin, the Bagh Complex, the MBO and the Flysch Belt (Mengal et al., 1994; Kakar et al., 2014). Triassic to Palaeocene sediments of the Indian Passive Margin (Kakar et al., 2014) are overthrust by the Mesozoic Bagh Complex along the Gawal Bagh thrust (Mengal et al., 1994). The Bagh Complex comprises a series of thrust bounded units, including a melange unit, two volcanic units (basalt-chert unit [Bbc], hyaloclastite-mudstone unit [Bhm]) and a sedimentary unit (Bs) [see Mengal et al. (1994) for detailed descriptions of each unit]. Thrusted over the Bagh Complex is the MBO (Kakar et al., 2014), described in more detail below. The uppermost unit is the Eocene to Holocene Flysch Belt that rests unconformably on top of the MBO and Bagh Complex in the Katawaz Basin (Mengal et al., 1994; Qayyum et al., 1996; Kasi et al., 2012). The Flysch Belt can be broadly divided into four thrust bounded formations (Nisai, Khujak, Multana and Bostan formations) comprising fluvial and deltaic successions (Qayyum et al., 1996; Kasi et al., 2012).

3.b. Muslim Bagh Ophiolite

The MBO is exposed as two massifs, the Saplai Tor Ghar and Jang Tor Ghar Massifs (Ahmad & Abbas, 1979; Mahmood et al., 1995; Gnos et al., 1997) (Fig. 1). The tectonic setting of formation of the MBO has been variously interpreted as a mid-ocean ridge (Mahmood et al., 1995), a back-arc basin (Siddiqui et al., 1996) or an island arc (M. Khan et al., 2007). However, most recently Kakar et al. (2014) have presented evidence that the MBO formed above a slow spreading supra-subduction zone, based on both the structure of the ophiolite and its arc-like geochemistry. Recent U-Pb dating of zircons in MBO plagiogranites by Kakar et al. (2012) gave a crystallisation age of 80.2 ± 1.5 Ma that is similar to ~82-81 Ma K-Ar ages obtained by Sawada et al. (1995). Dating of amphiboles from the sub-ophiolitic metamorphic sole have yielded K-Ar and plateau Ar/Ar ages of 80.5 ± 5.3 Ma (Sawada et al., 1995) and 70.7 ± 5 Ma (Mahmood et al., 1995), respectively. The younger age of 70.7 ± 5 Ma (Mahmood et al., 1995) is interpreted to date the age of emplacement of the MBO which, when taken in conjunction with the crystallisation age of the ophiolite, suggests that the ophiolite was obducted soon after formation (e.g., Kakar et al., 2014).

The Saplai Tor Ghar Massif displays a near-complete ophiolite sequence (Kakar et al., 2014), with only the extrusive basalts absent (Mahmood et al., 1995). The Jang Tor Ghar Massif however, only preserves mantle sequence rocks (i.e., foliated peridotite) of the oceanic lithosphere (Mahmood et al., 1995; Kakar et al., 2014). The mantle sequence of the MBO has been divided into a foliated peridotite section and mantle-crust transition zone (Kakar et al., 2014). The foliated peridotite is located in both massifs, and comprises serpentinised harzburgite with minor dunite and chromite deposits (Mahmood et al., 1995; M. Khan et al., 2007; Kakar et al., 2014). Lherzolite is also found in the lower part of the mantle sequence (Kakar et al., 2014). The mantle-crust transition zone of the MBO is a dunite-rich zone with minor gabbro, wherlite, pyroxenite and chromite only exposed in the Saplai Tor Ghar Massif (Mahmood et al., 1995; M. Khan et al., 2007; S. D. Khan et al., 2007; Kakar et al., 2014). Chromite bodies of the transition zone are larger than those in the foliated peridotite section of the mantle sequence (Kakar et al., 2014).

The oceanic crustal sequence, as exposed in the Saplai Tor Ghar Massif, comprises a 200 – 1500 m thick ultramafic-mafic cumulate zone (Ahmad & Abbas, 1979; Siddiqui et al., 1996) and a 1 km thick, poorly developed sheeted dyke complex (Siddiqui et al., 1996; M. Khan et al., 2007). The ultramafic-mafic cumulate zone displays both single and cyclic sequences grading from basal dunite, through pyroxenite, to gabbro, with infrequent anorthosite at the top of the cumulate zone (Ahmad & Abbas, 1979; Siddiqui et al., 1996; Kakar et al., 2014; M. Khan et al., 2007; Kakar et al., 2014). Above the cumulate zone, the sheeted dykes are doleritic, dioritic and plagiogranitic in composition and all display greenschist to amphibolite grade metamorphism (Sawada et al., 1995; Kakar et al., 2014).

Plagiogranites of the MBO are exclusively located at the base and middle portions of the sheeted dyke complex (Mahmood et al., 1995; Siddiqui et al., 1996). The plagiogranites are rare, comprising <5% by volume of the sheeted dyke complex, and take the form of dykes and small lenses (Fig. 2). They are discontinuous, intrusive bodies, sometimes tapering, displaying a range of sizes. Lenses range from 0.1×0.3 m to 1.0×3.0 m, with more dyke-like bodies ranging from 0.3×1.0 m to 1.5×3.0 m. The plagiogranites have sharp contacts with the enclosing sheeted dykes, and have also undergone greenschist-amphibolite facies metamorphism with foliated to mylonitised textures (Sawada et al., 1995; Siddiqui et al., 1996; Kakar et al., 2014). Samples for the current study were collected from a range of separate plagiogranite dykes and lenses from across the region. The general sampling locality is shown on Figure 1 with more detailed localities and sample information given in online Supplementary Material A at http://journals.cambridge.org/geo.

4. Petrography

The plagiogranites sampled from the MBO for the current study are predominately composed of quartz (~40 vol.%) and plagioclase (~50 vol.%), with hornblende and pyroxene comprising minor amounts (<<10 vol.%; hornblende > pyroxene), and zircon and Fe-Ti oxides common as accessory phases. Phenocryst phases of plagioclase, quartz, hornblende and pyroxene are surrounded by a fine groundmass composed of plagioclase, quartz, hornblende, pyroxene, potassium feldspar (rare), and accessory phases. All phenocryst phases have sub-hedral to anhedral crystal shapes, with plagioclase displaying simple and albite twinning, while hornblende twinning is rare. Throughout the sections, quartz is composed of sub-grains. However, unlike Coleman & Peterman's (1975) original definition of oceanic plagiogranites, the MBO plagiogranites do not display vermicular intergrowths of quartz and plagioclase. Evidence for hydrothermal alteration and low-grade metamorphism includes moderate sericitisation of plagioclase crystals (concentrated in the core of crystals; Fig. S1, online Supplementary Material B at http://journals.cambridge.org/geo).

5. Geochemical results

5.a. Analytical techniques

Plagiogranite samples were prepared and analysed for major, minor and trace elements at the School of Earth and Ocean Sciences, Cardiff University, Wales, U.K. Loss on ignition (LOI) was measured using ~1.5 ± 0.0001g of sample powder baked at 900°C in a Vecstar Furnace for 2 hours. Major and minor elements and Sc were measured using a JY-Horiba Ultima 2 Inductively Coupled Plasma Optical Emission Spectrometry (ICP-OES). Minor, trace and the rare earth elements (REE) were measured using a thermoelemental X series (X7) Inductively Coupled Plasma Mass Spectrometry (ICP-MS) following methods described by McDonald and Viljoen (2006). Accuracy and precision of the data were assessed using the international standard reference materials JB1a, JA2 and JG-3 (obtained analysis, certified values and detection limits for JB1a are shown in Table S1, online Supplementary Material C at http://journals.cambridge.org/geo). The full data set of plagiogranite samples are shown in Table 1.

5.b. Element mobility

The altered nature of the plagiogranite samples means that some of the major elements and large ion lithophile elements (LILE) may have been mobilised relative to the high field strength elements (HFSE) and REE (e.g., Hastie et al., 2007). Although low LOI values (0.59 – 2.45 wt. %) suggest that the plagiogranites have suffered little alteration, the high proportion of quartz (~40%) means that the effective LOI of the non-quartz components may double the whole rock values. However, major element (vs. LOI) variation plots of the plagiogranite samples show no correlation with LOI, all displaying very low R^2 values (see Fig. S1 of Supplementary Material C at http://journals.cambridge.org/geo). With the exception of MgO (<0.52), all major elements display R^2 values of <0.32. These data suggest that the major element concentrations are not primarily controlled by alteration, and can confidently be used to compare to literature Archean TTG data. Additionally, Sr (vs. LOI; Fig. S2, online Supplementary Material C at http://journals.cambridge.org/geo) also displays a very low R^2 value of <0.45. Consequently, the following discussion concentrates on the major elements and HFSE and REE, generally regarded as relatively immobile up to greenschist facies (e.g., Floyd & Winchester, 1975; Pearce & Peate, 1995; Hastie et al., 2007, 2009).

5.c. Major elements

The plagiogranites display a relatively narrow, high-SiO_2 range [70.8 – 80.2 wt.% (anhydrous values)], with most also having relatively high Al_2O_3 (10.7 – 15.8 wt.%) and Na_2O (1.7 – 4.5 wt.%) contents (Fig. 3). Samples have low TiO_2 (<0.4 wt.%), MgO (0.1 – 1.8 wt.%) and K_2O (<1.1 wt.%). $Al_2O_{3,}$ MnO (not shown), MgO and K_2O decrease with increasing SiO_2, while other oxides, such as TiO_2, Na_2O, $Fe_2O_{3(T)}$ and CaO show little to no correlation (Fig. 3). Also, the plagiogranites do not fall on clear liquid lines of descent along with the gabbros and sheeted dykes of the MBO. On a normative ternary An-Ab-Or plot, the plagiogranites classify as tonalites and trondhjemites (Fig. 4).

The major element abundances of the plagiogranites are very similar to those of Archean TTG (Condie, 2005; Martin et al., 2005; Moyen and Martin, 2012); with TTG compositions consistently plotting at the lower SiO_2 end of the plagiogranite compositions (Fig. 3). However, this similarity is not observed in K_2O contents, with TTG generally having much higher K_2O contents (1.65 – 2.22 wt. %) compared to the MBO plagiogranites (<1.1 wt. %).

5.d. Trace elements

The plagiogranites show no convincing intra-formation fractionation trends on trace element variation plots (Fig. 5). This is not surprising considering that the samples are collected from a diverse range of geographically distinct dykes and lenses. The plagiogranites span a wide range in Zr concentrations (~20 – 280 ppm); however, the majority of samples fall in the range 20 – 90 ppm, with only three having higher concentrations (130, 199, 283 ppm) suggestive of zircon accumulation (e.g., Rollinson, 2009). In general, the plagiogranites have lower trace element concentrations than the sheeted dyke complex of the MBO and, with the exception of Sr, have trace element contents similar to, or slightly greater than, the majority of the gabbros of the crustal section of the ophiolite (Fig. 5). As is the case with the major elements (Fig. 3), the plagiogranites also do not fall on clear liquid lines of descent along with the gabbros and sheeted dykes of the MBO (Fig. 5). As seen above, the major element compositions of the MBO plagiogranites are very similar to those of TTG compositions (Fig. 3); however, this similarity is not as evident in the trace elements (Fig. 5).

The plagiogranites show broadly coherent trends in the middle- to heavy-REE (M/HREE) on chondrite-normalised REE plots, but have variable light-REE (LREE) contents, from markedly enriched to relatively depleted patterns [e.g., 4.8 – 0.7 $(La/Sm)_N$] (Fig. 6a, c). The LREE enriched patterns shown by the majority of the plagiogranite samples are inconsistent with the original definition of plagiogranites (Coleman & Peterman, 1975), and are shown to be enriched relative to the well-studied crustal plagiogranites from the Oman and Troodos Ophiolites (Fig. 6a). However, plagiogranites from the Sjenica (Milovanovic et al., 2012) and Tasriwine Ophiolites (Samson et al., 2004) have recently been reported that have LREE enriched patterns (Fig. 6a). When compared to Archean TTG compositions, plagiogranite samples are mostly shown to not be as enriched in the LREE (Fig. 6a). Most samples also show a slight chondrite normalised enrichment in the heaviest REE relative to the MREE and display small U-shaped (concave upwards) patterns. The U-shaped patterns can be quantified using the Dy/Dy* ratio of Davidson et al. (2012), which ranges from 0.96 – 0.43 (Fig. 6b). Most plagiogranites have weak positive Eu anomalies [1.06 – 1.51 (Eu/Eu)*], with only three samples having negative Eu anomalies [0.74 – 0.94] (Fig. 6c). Interestingly, two of the three samples with negative Eu anomalies are also significantly enriched in the LREE.

On normal mid-ocean ridge basalt (N-MORB) normalised multi-element plots, most plagiogranites display relatively flat patterns at concentrations just below N-MORB, with positive Th anomalies and negative Nb-Ta-Ti anomalies (Fig. 7a). Zr and Hf contents vary from enriched to depleted, relative to N-MORB. Most samples also have positive Sr anomalies; however three samples have negative Sr anomalies, two of which display corresponding negative Eu anomalies (Fig. 6c).

6. Discussion

The modal abundance of quartz and plagioclase in combination with the low K_2O contents (<1.1 wt.%) of the MBO plagiogranites is similar to oceanic plagiogranites found elsewhere (e.g., Gerlach et al., 1981; Amri et al., 1996; Rollinson, 2009). Additionally, the trace element compositions of plagiogranites from the Muslim Bagh, Oman and Troodos Ophiolites all show a high degree of compositional overlap (Fig. 7a, plagiogranite field) (Rollinson et al., 2009; Freund et al., 2014). Nevertheless, the LREE-enriched and slightly concave-upward MREE patterns of the majority of MBO samples are distinct relative to the original oceanic plagiogranite definition (Coleman & Peterman, 1975; Coleman & Donato, 1979).

High SiO_2 (>70 wt.%) and Na_2O ($3 < Na_2O < 4.5$ wt.%) concentrations and low modal K-feldspar contents, low K_2O/Na_2O ratios and low Fe_2O_3+MgO+MnO+TiO_2 (most <5 wt.%) of the MBO plagiogranites make them compositionally similar to Archean TTG as defined by Martin et al. (2005) and Moyen and Martin (2012). Additionally, when compared to Archean TTG compositions on an N-MORB normalised multi-element plot, the plagiogranites display broadly similar concentrations, overlapping the TTG field at the lower LREE and higher HREE concentrations (Fig. 7b).

6.a. Plagiogranite petrogenesis

The majority of plagiogranites display enrichment in the LREE relative to the HREE (Fig. 6c) and all plagiogranites have negative Nb-Ta and positive Th anomalies (Fig. 7a). Additionally, the N-MORB-like concentrations of the other trace elements suggest that the plagiogranites (Fig. 6c) were generated at a MOR setting with a subduction input, likely a supra-subduction zone. This supports recent work by Kakar et al. (2014) who propose a supra-subduction model for the formation of the MBO. However, the petrogenesis of oceanic plagiogranites is controversial with fractional crystallisation, partial melting or silicate – liquid immiscibility being variously proposed as petrogenetic models [see Koepke et al. (2007) for a review]. Below, we discuss the implications the plagiogranite compositions have for each of the possible petrogenetic models.

6.a.1. Fractional crystallisation and liquid immiscibility

The layered gabbros and sheeted dykes of the MBO crustal section represent possible cumulates and parental melts, respectively from which to derive the plagiogranites by crystallisation. However, major and trace element variation diagrams (Fig. 3**,** 5) show that the plagiogranites do not plot along the same liquid lines of descent as any of the other MBO units. The fact that the plagiogranites define their own distinct field clearly indicates that they are not related to the other units by simple fractional crystallisation processes. The lack of intermediate units within the ophiolite sequence also argues against an origin for the plagiogranites by fractional crystallisation from a basic parental melt. Additionally, the narrow SiO_2 range of the plagiogranites would suggest fractional crystallisation did not play a primary role in their petrogenesis.

Concave-upwards patterns displayed by the plagiogranites (Fig. 6c) support a role for amphibole during their petrogenesis; a result of amphiboles preference for the MREE over the LREE and HREE (e.g., Davidson et al., 2012). However, the concave-upward pattern on its own does not indicate whether amphibole was crystallising from a parental magma or acting as a residual phase during the fusion of a mafic protolith.

An origin by silicate-liquid immiscibility (e.g., Dixon & Rutherford, 1979) is also unlikely for the MBO plagiogranites. This is evidenced by the absence of the associated immiscible Fe-rich liquid (as Fe-rich mafic units) from the MBO.

6.a.2. Partial melting

Experimental work of Koepke et al. (2004) and France et al. (2010) has shown that low TiO_2 contents (<1 wt.%; Koepke et al., 2004) are characteristic of oceanic plagiogranites derived through partial melting a mafic protolith; a consequence of the gabbroic protoliths having initially low TiO_2 contents, typical of cumulate gabbros of the oceanic crust (Koepke et al., 2004, 2007). Low TiO_2 contents of the MBO plagiogranites (Fig. 3b) are similar to those in the experimentally derived high-SiO_2 melts of Koepke et al. (2004), suggesting they were derived by partial melting of a gabbroic protolith in the crustal sequence of the MBO. In addition, TiO_2 contents of the MBO plagiogranites plot below the boundary line drawn by Koepke et al. (2007) that separates plagiogranites derived by hydrous partial melting (plot below black dashed line, Fig. 3b) from those plagiogranites derived by crystallisation or immiscibility processes (plot above black dashed line).

Additionally, as shown in Figure 3, major element concentrations of the MBO plagiogranites are similar to Archean TTG (Condie, 2005; Martin et al., 2005; Moyen and Martin, 2012), which are generally regarded to have been generated through partial melting of a mafic igneous protolith (e.g., Drummond et al., 1996; Foley et al., 2002; Rapp et al., 2003; Martin et al., 2005; Moyen & Stevens, 2006; Nutman et al., 2009; Hastie et al., 2015, 2016). We suggest that the lower K_2O contents displayed by the plagiogranites, compared to Archean TTG, is the result of the TTG rocks being derived from a more primitive mantle prior to continental crust extraction, and therefore a less depleted mantle than the present. Trace element variation plots (Fig. 5) however do not show as convincing a similarity between the MBO plagiogranites and Archean TTG as do the major element variation plots (Fig. 3). Nevertheless, overall the MBO plagiogranites have broadly similar trace element compositions to Archean TTG (Fig. 7b).

Negative Eu and Sr anomalies (Fig. 6c, 7a) and decreasing Al_2O_3 with increasing SiO_2 (Fig. 3) in some samples could potentially be explained by a small amount of late stage plagioclase fractional crystallisation. However, negative Eu and Sr anomalies can also be the result of plagioclase in the melting residue, while the decrease in Al_2O_3 with SiO_2 can be reproduced through small degrees of partial melting as demonstrated by Beard & Lofgren (1991). In the following section we will use trace element modelling to test a partial melting model for the MBO plagiogranites.

6.b. Modelling of partial melting

To model the partial melting of a mafic protolith the non-modal batch melting equation of Shaw (1970) was used for the calculations:

$$C_l = \frac{\mathrm{C}_0}{\mathrm{D}_0 + F(1-P)} \qquad [1]$$

where, C_l is the concentration of a particular trace element in a resultant melt, C_0 is the concentration of an element in the source region prior to partial melting, F is the mass fraction of melt generated, D_0 is the bulk partition coefficient of an element prior to partial melting and P is the partition coefficient of an element weighted by the proportion contributed by each mineral phase to the melt. Hornblende gabbro, C51 [from Kakar et al. (2014)] was used as the protolith. This sample was collected from the cumulate sequence of the crustal section of the MBO and was chosen as the protolith since the concave-upward pattern shown by the plagiogranites suggests that amphibole may have been left behind in the melting residue. The partition coefficients used are those for elements in equilibrium with TTG-like silicic melts from Bedard (2006). Mineral modes of the hornblende gabbro are those of Kakar et al. (2014) and Siddiqui et al. (1996). Melt modes were calculated using 1 kbar experimental runs from Beard & Lofgren (1991) as they provide enough petrological information to carry out the calculation. Melting was stopped at 14.5%, as this is the point at which hornblende is exhausted from the protolith. Mineral and melt modes, partition coefficients, hornblende gabbro starting composition and model results can be found in Table S1, online Supplementary Material D at http://journals.cambridge.org/geo.

Figure 7c shows that the incompatible trace element patterns (including negative Nb and Ti anomalies and positive Th and Zr anomalies) of the plagiogranites can be replicated by 5 – 10% partial melting of the hornblende gabbro. Nonetheless the modelling generates a larger negative Sr anomaly than seen in the MBO plagiogranites. This result is attributed to the use of a high Sr partition coefficient in plagioclase (6.65; Bedard, 2006) and this discrepancy can be removed if a lower partition coefficient is used [i.e., 3, based on the range reported by Laurent et al. (2013)].

Despite the evidence supporting a partial melting model for the MBO plagiogranites, the reason behind the negative K_2O trend displayed by the plagiogranites when plotted against SiO_2 (Fig. 3) is uncertain. It is possible however that the negative trends displayed by both K_2O and Al_2O_3 are the result of an interplay between fractional crystallisation (plagioclase and biotite(?)) and/or varying degrees of partial melting and source variation.

6.c. Comparison with other Tethyan Ophiolite plagiogranites and implications for the tectonomagmatic setting of the Muslim Bagh Ophiolite

As we have shown, some geochemical characteristics of the MBO plagiogranites (i.e., LREE enriched and concave-upward MREE patterns) do not conform to the definition of oceanic plagiogranites as proposed by Coleman & Peterman (1975). The results from this study are similar to previous plagiogranite analyses from the MBO presented by Kakar et al. (2014), who also report MBO plagiogranites with LREE enriched patterns [1 – 7, $(La/Sm)_N$], as well as negative Nb-Ta-Ti anomalies and low TiO_2 contents ($\leq$0.20 wt. %).

The MBO plagiogranites are significantly different to those from other Tethyan Ophiolites in terms of both field and geochemical characteristics. First, LREE contents of Troodos and Oman Ophiolite crustal plagiogranites are relatively depleted compared to the HREE (Fig. 6a) (Rollinson et al., 2009; Freund et al., 2014) and therefore a more depleted source is required for these plagiogranites relative to the MBO plagiogranites. It is however beyond the scope of this study to investigate further the difference in source enrichment between the MBO plagiogranites and those plagiogranites situated in the Oman and Troodos Ophiolites. Secondly, the plagiogranites of the MBO are solely located in the crustal section of the ophiolite, whereas geochemically distinct groups of plagiogranites have been identified in crust and mantle sections of the Troodos and Oman Ophiolites (Rollinson, 2009, 2014; Freund et al., 2014). Thirdly, the MBO plagiogranites are generally smaller intrusive bodies (on a scale of no more than a few meters) than those found in both the Troodos and Oman Ophiolites, where plagiogranites range from several tens of meters to kilometre sized plutons (Rollinson et al., 2009; Freund et al., 2014).

The poorly developed sheeted dyke complex (M. Khan et al., 2007; Kakar et al., 2014) of the MBO crustal section is likely the result of the imbalance between spreading rate and magma supply in a supra-subduction zone tectonic setting (Robinson et al., 2008). Robinson et al. (2008) have proposed that both the forearc and backarc of a supra-subduction zone generally experience lower magma supply rates, due to eruptions at the volcanic arc, and high extensional strain rates. Therefore, the small size, restricted distribution and lack of geochemical variability (i.e., uniform composition) amongst the MBO plagiogranites could be a result of this decreased magma supply in the supra-subduction zone where the MBO crystallised. Consequently, the decreased magma supply results in a small degree of partial melting of the plagiogranite source (i.e., crustal hornblende gabbros).

6.d. Implications for Archean TTG genesis

Most previous and current research into Archean TTG petrogenesis favours models in which juvenile Archean continental crust is generated by partial melting of mafic igneous protoliths (e.g., Sen & Dunn, 1994; Wolf & Wyllie, 1994; Foley et al., 2002; Rapp et al., 2003; Moyen & Stevens, 2006; Laurie & Stevens, 2012; Zhang et al., 2013; Ziaja et al., 2014; Hastie et al., 2016), the setting of which is still controversial, with both subduction/flat slab subduction/underthrusting (e.g., Drummond et al., 1996; Martin et al., 2005; Nutman et al., 2009; Hastie et al., 2015) and intracrustal (Hamilton, 1998; Hawkesworth et al., 2016) settings having been proposed for the derivation of Archean TTG of various ages.

Since the original definition of oceanic plagiogranites in the mid-1970s by Coleman & Peterman (1975), oceanic plagiogranites have been shown to differ compositionally to Archean TTG; being less potassic, and having MORB-like LREE and flat HREE patterns. Numerous studies on oceanic plagiogranites from the Oman Ophiolite (Rollinson, 2008, 2009, 2014) have suggested that although the Oman Ophiolite plagiogranites have compositions that are similar to oceanic plagiogranites [as defined by Coleman & Peterman (1975)] and differ compositionally from Archean TTG, they can be instructive on Archean TTG genesis. Rollinson (2009) noted that in addition to the conditions of plagiogranite petrogenesis, a source region enriched in the LREE is also required in order to generate the LREE-enriched nature of Archean TTG. Additionally, Rollinson (2008) has suggested that trondhjemite (plagiogranite) petrogenesis in the Oman Ophiolite acts as a possible analogue for the generation of Earth's first felsic crust in the Hadean. Rollinson (2008) has argued that early (Hadean) felsic crust was of low volume and this corresponds to the low volume of plagiogranites we see in recent ophiolite sequences.

The MBO plagiogranites are compositionally different (LREE-enriched and concave-upward MREE patterns) to the original oceanic plagiogranite definition, but are geochemically similar to Archean TTG (e.g., Condie, 2005; Martin et al., 2005; Moyen and Martin, 2012) (Fig. 3, 7b). Consequently, the MBO plagiogranites can be used as a recent (Late Cretaceous) analogue to investigate the formation of some Archean TTG rocks.

The MBO plagiogranites are found within mafic crust that was formed at a convergent margin – specifically the upper plate above the subduction zone (e.g., Siddiqui et al., 1996, 2011; Kakar et al., 2014). The similarity in composition between the MBO plagiogranites and Archean TTG suggests that some of the earliest silicic continental crust may have been derived from melting the overriding plates in primitive subduction-like zones. We acknowledge that there is a contrast in volume between the MBO plagiogranites and Archean TTG; however, we infer that the genesis of these plagiogranites can be instructive on the generation of some, but not all, Archean TTG. In addition, the overall greater enrichment in the LREE relative to the HREE of Archean TTG compared to the MBO plagiogranites suggests that to source a larger portion of Archean TTG requires a slightly more enriched source than that of the MBO plagiogranites (e.g., Rollinson, 2009). Again, this could possibly be due to the extraction of continental crust, and depletion of the mantle over time.

7. Conclusions

1. Oceanic plagiogranites of the MBO are exclusively located at the base and middle portions of the sheeted dyke complex, where they form small, intrusive dyke-like bodies and lenses.
2. Low TiO_2 contents (<0.4 wt. %) in the plagiogranites and a lack of intermediate rocks in the sheeted dyke complex suggest an origin by partial melting of mafic rocks. This is confirmed by batch melt trace element modelling of a crustal hornblende gabbro from the crustal sequence of the MBO. This modelling shows that the plagiogranites can be replicated by 5 – 10% partial melting, possibly with a small degree of late stage fractional crystallisation of plagioclase(?) to account for negative Sr and Eu anomalies and a decrease in Al_2O_3 with SiO_2.
3. The similarity in composition of the MBO plagiogranites with Archean TTG rocks supports the model that some Archean TTG could be generated by partial melting of a mafic protolith, possibly in the overriding plate of a subduction-like zone.

Acknowledgements:

Iain McDonald is thanked for the major and trace element analyses of the samples. We also thank Ahmed Shah, Inayatullah and Akbar for assistance during field work. The Volcanology Igneous Petrology Experimental Research (VIPER) Workshop of the University of Birmingham is thanked for access for petrological study of the samples. Hugh Rollinson is thanked for comments on an earlier draft which substantially improved the manuscript. S. Nasir, S. Köksal and an anonymous reviewer are also thanked for their carefully thought out and well-structured reviews which have improved the manuscript. This research received no specific grant from any funding agency, commercial or not-for-profit sectors.

Declaration of Interest: None.

References

Ahmad, Z., Abbas, S. G., 1979. The Muslim Bagh Ophiolites, in: Farah, A., DeJong, A. (Eds.), Geodynamics of Pakistan. Geological Survey of Pakistan, Pakistan, pp. 243–251.

Amri, I., Benoit, M., Ceuleneer, G., 1996. Tectonic setting for the genesis of oceanic plagiogranites: evidence from a paleo-spreading structure in the Oman Ophiolite. Earth and Planetary Science Letters 139, 177–194.

Aranovich, L. Y., Bortnikov, N. S., Serebryakov, N. S., Sharkov, E. V., 2010. Conditions of the formation of plagiogranite from the Markov Trough, Mid-Atlantic Ridge, 5°52′-6°02′N. Doklady Earth Sciences 434, 1257–1262.

Asrarullah, Ahmad, Z., Abbas, S. G., 1979. Ophiolites in Pakistan: an introduction, in: Farah, A., DeJong, A. (Eds.), Geodynamics of Pakistan. Geological Survey of Pakistan, Pakistan, pp. 181–192.

Barker, F., 1979. Trondhjemite: definition, environment and hypothesis of origin, in: Barker, F. (Ed.), trondhjemites, dacites, and related rocks. Elsevier, Amsterdam, pp. 1–12.

Beard, J. S., Lofgren, G. E., 1991. Dehydration melting and water-saturated melting of basaltic and andesitic greenstones and amphibolites at 1, 3 and 6.9 kb. Journal of Petrology 32, 365–401.

Bedard, J. H., 2006. A catalytic delamination-driven model for coupled genesis of Archean crust and sub-continental lithospheric mantle. Geochimica et Cosmochimica Acta 70, 1188–1214.

Coleman, R. G., Donato, M. M., 1979. Oceanic plagiogranite revisited, in: Barker, F. (Ed.), trondhjemites, dacites, and related rocks. Elsevier, Amsterdam, pp. 149–168.

Coleman, R. G., Peterman, Z. E., 1975. Oceanic plagiogranite. Journal of Geophysical Research 80, 1099–1108.

Condie, K. C., 2005. TTGs and adakites: Are they both slab melts? Lithos 80, 33–44.

Davidson, J., Turner, S., Plank, T., 2012. Dy/Dy*: Variations arising from mantle sources and petrogenetic processes. Journal of Petrology 54, 525–537.

Dick, H. J. B., Natland, J. H., Alt, J. C., Bach, W., Bideau, D., Gee, J. S., Haggas, S., Hertogen, J. G. H., Hirth, G., Holm, P. M., Ildefonse, B., Iturrino, G. J., John, B. E., Kelley, D. S., Kikawa, E., Kingdon, A., LeRoux, P. J., Maeda, J., Meyer, P. S., Miller, J., Naslund, H. R., Niu, Y. -L., Robinson, P. T., Snow, J., Stephen, R. A., Trimby, P. W., Worm, H. -U., Yoshinobu, A., 2000. A long in situ section of the lower crust: results of ODP Leg 176 drilling at the Southwest Indian Ridge. Earth and Planetary Science Letters 179, 31–51.

Dixon, S., Rutherford, M. J., 1979. Plagiogranites as late-stage immiscible liquids in ophiolite and mid-ocean ridge suites an experimental study. Earth and Planetary Science Letters 45, 45–60.

Drummond, M. S., Defant, M. J., Kepezhinskas, P. K., 1996. Petrogenesis of slab-derived trondhjemite-tonalite-dacite/adakite magmas. Transactions of the Royal Society of

Edinburgh 87, 205–215.

Erdmann, M., Fischer, L. A., France, L., Zhang, C., Godard, M., Koepke, J., 2015. Anatexis at the roof of an oceanic magma chamber at IODP Site 1256 (equatorial Pacific): an experimental study. Contributions to Mineralogy and Petrology 169, 1–28.

Flagler, P. A., Spray, J. G., 1991. Generation of plagiogranite by amphibolite anatexis in oceanic shear zones. Geology 19, 70–73.

Floyd, P. A., Winchester, J. A., 1975. Magma type and tectonic setting discrimination using immobile elements. Earth and Planetary Science Letters 27, 211–218.

Foley, S. F., Tiepolo, M., Vannucci, R., 2002. Growth of early continental crust controlled by melting of amphibolite in subduction zones. Nature 417, 837–840.

France, L., Ildefonse, B., Koepke, J., 2009. Interactions between magma and hydrothermal system in Oman Ophiolite and in IODP Hole 1256D: fossilization of a dynamic melt lens at fast spreading ridges. Geochemistry, Geophysics, Geosystems 10, 1–30.

France, L., Koepke, J., Ildefonse, B., Cichy, S. B., Deschamps, F., 2010. Hydrous partial melting in the sheeted dike complex at fast spreading ridges: experimental and natural observations. Contributions to Mineralogy and Petrology 160, 683-704.

Freund, S., Haase, K. M., Keith, M., Beier, C., Garbe-Schonberg, D., 2014. Constraints on the formation of geochemically variable plagiogranite intrusions in the Troodos Ophiolite, Cyprus. Contributions to Mineralogy and Petrology 167, 1–22.

Gerlach, D. C., Leeman, W. P., Ave Lallemant, H .G., 1981. Petrology and geochemistry of plagiogranite in the Canyon Mountain Ophiolite, Oregon. Contributions to Mineralogy and Petrology 77, 82–92.

Gillis, K. M., Coogan, L. A, 2002. Anatectic migmatites from the roof of an ocean ridge magma chamber. Journal of Petrology 43, 2075–2095.

Gnos, E., Immenhauser, A., Peters, T., 1997. Late Cretaceous/early Tertiary convergence between the Indian and Arabian plates recorded in ophiolites and related sediments. Tectonophysics 271, 1–19.

Grimes, C. B., Ushikubo, T., John, B. E., Valley, J. W., 2011. Uniformly mantle-like Delta18O in zircons from oceanic plagiogranites and gabbros. Contributions to Mineralogy and Petrology 161, 13–33.

Hamilton, W. B., 1998. Archean magmatism and deformation were not products of plate tectonics. Precambrian Research 91, 143–179.

Hastie, A. R., Fitton, J. G., Bromiley, G. D., Butler, I. B., Odling, N. W. A., 2016. The origin of Earth's first continents and the onset of plate tectonics. Geology 44, 855–858.

Hastie, A. R., Fitton, J. G., Mitchell, S. F., Neill, I., M. Nowell, G., Millar, I. L., 2015. Can fractional crystallization, mixing and assimilation processes be responsible for Jamaican-type adakites? Implications for generating EoArchean continental crust. Journal of Petrology 56, 1251–1284.

Hastie, A. R., Kerr, A. C., Mitchell, S. F., Millar, I. L., 2009. Geochemistry and tectonomagmatic significance of lower Cretaceous island arc lavas from the Devils Racecourse Formation, eastern Jamaica. Geological Society, London, Special Publications 328, 339–360.

Hastie, A. R., Kerr, A. C., Pearce, J. A., Mitchell, S. F., 2007. Classification of altered volcanic island arc rocks using immobile trace elements: development of the Th-Co discrimination diagram. Journal of Petrology 48, 2341–2357.

Hawkesworth, C. J., Cawood, P. A., Dhuime, B., 2016. Tectonics and crustal evolution. GSA Today 26, 4–11.

Jafri, S. H., Charan, S. N., Govil, P. K., 1995. Plagiogranite from the Andaman Ophiolite Belt, Bay of Bengal, India. Journal of the Geological Society, London 152, 681–687.

Kakar, M. I., Collins, A. S., Mahmood, K., Foden, J. D., Khan, M., 2012. U-Pb zircon crystallization age of the Muslim Bagh Ophiolite: Enigmatic remains of an extensive pre-Himalayan arc. Geology 40, 1099–1102.

Kakar, M. I., Kerr, A. C., Mahmood, K., Collins, A. S., Khan, M., McDonald, I., 2014. Supra-subduction zone tectonic setting of the Muslim Bagh Ophiolite, northwestern Pakistan: Insights from geochemistry and petrology. Lithos 202–203, 190–206.

Kasi, A. K., Kassi, A. M., Umar, M., Manan, R. A., Kakar, M. I., 2012. Revised lithostratigraphy of the Pishin Belt, northwestern Pakistan. Journal of Himalayan Earth Sciences 45, 53–65.

Kaur, G., Mehta, P. K., 2005. The Gothara plagiogranite: evidence for oceanic magmatism in a non-ophiolitic association, North Khetri Copper Belt, Rajasthan, India? Journal of Asian Earth Sciences 25, 805–819.

Kerrich, R., Polat, A., 2006. Archean greenstone-tonalite duality: Thermochemical mantle convection models or plate tectonics in the early Earth global dynamics? Tectonophysics 415, 141–165.

Khan, M., Kerr, A. C., Mahmood, K., 2007. Formation and tectonic evolution of the Cretaceous-Jurassic Muslim Bagh ophiolitic complex, Pakistan: implications for the composite tectonic setting of ophiolites. Journal of Asian Earth Sciences 31, 112–127.

Khan, S. D., Mahmood, K., Casey, J. F., 2007. Mapping of Muslim Bagh ophiolite complex (Pakistan) using new remote sensing, and field data. Journal of Asian Earth Sciences 30, 333–343.

Khan, S. D., Walker, D. J., Hall, S. A., Burke, K. C., Shah, M. T., Stockli, L., 2009. Did the Kohistan-Ladakh island arc collide first with India? Bulletin of the Geological Society of America 121, 366–384.

Koepke, J., Berndt, J., Feig, S. T., Holtz, F., 2007. The formation of SiO2-rich melts within the deep oceanic crust by hydrous partial melting of gabbros. Contributions to

Mineralogy and Petrology 153, 67–84.

Koepke, J., Feig, S. T., Snow, J., Freise, M., 2004. Petrogenesis of oceanic plagiogranites by partial melting of gabbros: an experimental study. Contributions to Mineralogy and Petrology 146, 414–432.

Kusky, T. M., Windley, B. F., Safonova, I., Wakita, K., Wakabayashi, J., Polat, A., Santosh, M., 2013. Recognition of ocean plate stratigraphy in accretionary orogens through Earth history: a record of 3.8billion years of sea floor spreading, subduction, and accretion. Gondwana Research 24, 501–547.

Laurent, O., Doucelance, R., Martin, H., Moyen, J. F., 2013. Differentiation of the late-Archean sanukitoid series and some implications for crustal growth: Insights from geochemical modelling on the Bulai pluton, Central Limpopo Belt, South Africa. Precambrian Research 227, 186–203.

Laurie, A., Stevens, G., 2012. Water-present eclogite melting to produce Earth's early felsic crust. Chemical Geology 314–317, 83–95.

Le Maitre, R. W., Streckeisen, A., Zanettin, B., Le Bas, M. J., Bonin, B., Bateman, P., Bellieni, G., Dudek, A., Efremova, S., Keller, J., Lameyre, J., Sabine, P. A., Schmid, R., Sorensen, H., Woolley, A. R., 2002. Igneous Rocks : A Classification and Glossary of Terms.

Mahmood, K., Boudier, F., Gnos, E., Monie, P., Nicolas, A., 1995. 40Ar/39Ar dating of the emplacement of the Muslim Bagh Ophiolite, Pakistan. Tectonophysics 250, 169–181.

Martin, H., Smithies, R. H., Rapp, R., Moyen, J. F., Champion, D., 2005. An overview of adakite, tonalite-trondhjemite-granodiorite (TTG), and sanukitoid: Relationships and some implications for crustal evolution. Lithos 79, 1–24.

McDonald, I., Viljoen, K. S., 2006. Platinum-group element geochemistry of mantle eclogites: a reconnaissance study of xenoliths from the Orapa kimberlite, Botswana.

Applied Earth Science 115, 81–93.

Mengal, J. M., Kimura, K., Siddiqui, R. H., Kojima, S., Naka, T., Bakht, M. S., Kamada, K., 1994. The lithology and structure of a Mesozoic sedimentary-igneous assemblage beneath the Muslim Bagh Ophiolite, northern Balochistan, Pakistan. Bulletin of the Geological Survey of Japan 2, 51–61.

Milovanovic, D., Sreckovic-Batocanin, D., Savic, M., Popovic, D., 2012. Petrology of plagiogranite from Sjenica, Dinaridic Ophiolite Belt (southwestern Serbia). Geologica Carpathica 63, 97–106.

Moyen, J. F., Martin, H., 2012. Forty years of TTG research. Lithos 148, 312–336.

Moyen, J. F., Stevens, G., 2006. Experimental constraints on TTG petrogenesis: implications for Archean geodynamics, in: Benn, K., Mareschal, J. -C., Condie, K. C. (Eds.), Archean geodynamics and environments. American Geophysical Union, Geophysical Monograph 164, Washington D.C., pp. 149–175.

Nakamura, K., Morishita, T., Chang, Q., Neo, N., Kumagai, H., 2007. Discovery of lanthanide tetrad effect in an oceanic plagiogranite from an ocean core complex at the Central Indian Ridge 25S. Geochemical Journal 41, 135–140.

Nutman, A. P., Bennett, V. C., Friend, C. R. L., Jenner, F., Wan, Y., Liu, D., 2009. EoArchean crustal growth in west Greenland (Itsaq Gneiss Complex) and in north-eastern China (Anshan area): review and synthesis. Geological Society, London, Special Publications 318, 127–154.

Pearce, J. A, Peate, D. W., 1995. Tectonic implications of the composition of volcanic arc magmas. Annual Review of Earth and Planetary Sciences 23, 251–285.

Qayyum, M., Niem, A. R., Lawrence, R. D., 1996. Newly discovered Paleogene deltaic sequence in Katawaz Basin, Pakistan, and its tectonic implications. Geology 24, 835–838.

Rao, D. R., Rai, H., Kumar, J. S., 2004. Origin of oceanic plagiogranite in the Nidar ophiolitic sequence of eastern Ladakh, India. Current Science 87, 999–1005.

Rapp, R. P., Shimizu, N., Norman, M. D., 2003. Growth of early continental crust by partial melting of eclogite. Nature 425, 605–609.

Robinson, P. T., Malpas, J., Dilek, Y., Zhou, M., 2008. The significance of sheeted dike complexes in ophiolites. GSA Today 18, 4–10.

Rollinson, H., 2014. Plagiogranites from the mantle section of the Oman Ophiolite: models for early crustal evolution. Geological Society, London, Special Publications 392, 247–261.

Rollinson, H., 2009. New models for the genesis of plagiogranites in the Oman Ophiolite. Lithos 112, 603–614.

Rollinson, H., 2008. Ophiolitic trondhjemites: a possible analogue for Hadean felsic “crust.” Terra Nova 20, 364–369.

Samson, S. D., Inglis, J. D., D’Lemos, R. S., Admou, H., Blichert-Toft, J., Hefferan, K., 2004. Geochronological, geochemical, and Nd-Hf isotopic constraints on the origin of Neoproterozoic plagiogranites in the Tasriwine Ophiolite, Anti-Atlas orogen, Morocco. Precambrian Research 135, 133–147.

Sawada, Y., Nagao, K., Siddiqui, R. H., Khan, S. R., 1995. K-Ar ages of the Mesozoic igneous and metamorphic rocks from the Muslim Bagh area, Pakistan. Proceedings of Geoscience Colloquium 12, 73–90.

Sen, C., Dunn, T., 1994. Dehydration melting of a basaltic composition amphibolite at 1.5 and 2.0 GPa: implications for the origin of adakites. Contributions to Mineralogy and Petrology 117, 394–409.

Shaw, D. M., 1970. Trace element fractionation during anatexis. Geochimica et Cosmochimica Acta 34, 237–243.

Siddiqui, R. H., Aziz, A., Mengal, J. M., Hoshino, K., Sawada, Y., 1996. Geology, petrochemistry and tectonic evolution of the Muslim Bagh Ophiolite Complex, Pakistan. Proceedings of Geoscience Colloquium 16, 11–46.

Siddiqui, R. H., Mengal, J. M., Hoshino, K., Sawada, Y., Brohi, I. A., 2011. Back-arc basin signatures represented by the sheeted dykes from the Muslim Bagh Ophiolite Complex, Balochistan, Pakistan. Sindh University Research Journal 43, 51–62.

Sun, S. -s., McDonough, W. F., 1989. Chemical and isotopic systematics of oceanic basalts: implications for mantle composition and processes. Geological Society, London, Special Publications 42, 313–345.

Tilton, G. R., Hopson, C. A., Wright, J. E., 1981. Uranium-lead isotopic ages of the Samail Ophiolite, Oman, with applications to Tethyan Ocean ridge tectonics. Journal of Geophysical Research: Solid Earth 86, 2763–2775.

Twining, K., 1996. Origin of plagiogranite in the Troodos ophiolite, Cyprus, in: 9th Keck Symposium in Geology. pp. 245–248.

Wolf, M. B., Wyllie, P. J., 1994. Dehydration-melting of amphibolite at 10 kbar: the effects of temperature and time. Contributions to Mineralogy and Petrology 115, 369–383.

Yaliniz, M. K., Floyd, P. A., Goncuoglu, M. C., 2000. Petrology and geotectonic significance of plagiogranite from the Sarikaraman Ophiolite (Central Anatolia, Turkey). Ofioliti 1, 31–37.

Zhang, C., Holtz, F., Koepke, J., Wolff, P. E., Ma, C., Bédard, J. H., 2013. Constraints from experimental melting of amphibolite on the depth of formation of garnet-rich restites, and implications for models of Early Archean crustal growth. Precambrian Research 231, 206–217.

Ziaja, K., Foley, S. F., White, R. W., Buhre, S., 2014. Metamorphism and melting of picritic crust in the early Earth. Lithos 189, 173–184.

Figure Captions

Figure 1. Geological map of the Muslim Bagh area. Inset highlights the location of the Muslim Bagh Ophiolite in north-western Pakistan (modified from Kakar et al., 2014).

Figure 2. Field photographs of the Muslim Bagh Ophiolite plagiogranites. Plagiogranites are exclusively located within the sheeted dyke complex of the ophiolite crustal sequence, where they take the form of dyke-like bodies (**a**), and lenses (**b**).

Figure 3. Major element variation plots (vs. SiO_2) of the Muslim Bagh Ophiolite plagiogranites. Also plotted are the sheeted dykes and gabbros of the crustal section of the Muslim Bagh Ophiolite (data from Kakar et al., 2014) and Archean TTG average compositions; C2005 (Condie, 2005), M2005 (Martin et al., 2005) and MM2012 (Moyen & Martin, 2012). The black dashed line in (b) separates plagiogranites derived by hydrous partial melting (below the line) and those plagiogranites derived through differentiation or liquid immiscibility (above the line) (after Koepke et al., 2007).

Figure 4. Normative An-Ab-Or ternary plot. Muslim Bagh Ophiolite plagiogranites classify as either tonalites or trondhjemites. Fields from Barker (1979).

Figure 5. Representative trace element variation plots of the Muslim Bagh Ophiolite plagiogranites. The sheeted dykes and gabbros of the crustal section of the Muslim Bagh Ophiolite (data from Kakar et al., 2014), and Archean TTG average compositions are also plotted; symbols and references as in Figure 3.

Figure 6. a) Plot of $(La/Sm)_N$ vs. $(Gd/Yb)_N$ highlighting the LREE enriched nature of the majority of the Muslim Bagh Ophiolite plagiogranites relative to the depleted Oman (Rollinson, 2009) and Troodos Ophiolites (Freund et al., 2014). Also plotted are LREE enriched plagiogranites from the Sjenica (Milovanovic et al., 2012) and Tasriwine Ophiolites (Samson et al., 2004) and Archean TTG average compositions (symbols and references as in Figure 3). b) Plot of Dy/Dy* vs. Dy/Yb showing the majority of the Muslim Bagh Ophiolite plagiogranites to plot in the concave-upward quadrant (black dotted lines) and follow the amphibole vector (arrow) in figure 4 of Davidson et al. (2012). The plot quantifies the degree of concavity, and supports a role for amphibole in the petrogenesis of the plagiogranites, either as a residual or crystallising phase. c) Chondrite normalised rare earth element plot of the Muslim Bagh Ophiolite plagiogranites. Normalising values after Sun & McDonough (1989).

Figure 7. a) Normal mid-ocean ridge basalt normalised multi-element plot of the Muslim Bagh Ophiolite plagiogranites. Dashed plagiogranites field represents analyses of plagiogranites from the Troodos (Freund et al., 2014) and Oman (Rollinson, 2009) Ophiolites. b) Normal mid-ocean ridge basalt normalised multi-element plot comparing the Muslim Bagh Ophiolite plagiogranites with Archean TTG average compositions (Condie, 2005; Martin et al., 2005; Moyen & Martin, 2012). c) Trace element modelling of batch melting. The primitive mantle normalised multi-element plot compares the trace element composition resulting from trace element melt modelling of a crustal hornblende gabbro with the composition of the Muslim Bagh Ophiolite plagiogranites. Plagiogranite compositions can be replicated by 5 – 10% partial melting of a hornblende gabbro. Dashed black lines represent melts derived by partial melting when using a lower (i.e., 3; Laurent et al., 2013)

partition coefficient for Sr in plagioclase. Normalising values after Sun & McDonough (1989).

Table 1. Major and trace element analyses of the Muslim Bagh Ophiolite plagiogranites

Sample	Pl-01	Pl-02	Pl-03	Pl-06	Pl-07	Pl-13	Pl-15	Pl-17	Pl-19	Pl-21	Pl-22	Pl-23	Pl-25
SiO_2 (wt. %)	73.08	70.71	70.26	70.00	71.66	72.06	72.40	74.06	74.85	74.69	72.56	79.73	76.85
TiO_2	0.30	0.31	0.30	0.34	0.30	0.31	0.34	0.30	0.29	0.29	0.39	0.10	0.28
Al_2O_3	12.98	14.83	14.87	15.50	15.63	15.03	13.37	10.50	13.42	13.79	14.41	12.27	11.68
Fe_2O_3 (t)	2.81	3.48	3.00	2.47	2.40	2.60	2.84	4.03	3.02	2.79	4.47	1.25	3.87
MnO	0.04	0.05	0.04	0.04	0.04	0.04	0.04	0.03	0.03	0.02	0.04	0.01	0.04
MgO	1.81	1.01	0.78	0.66	0.63	0.42	0.92	1.22	0.50	0.40	0.37	0.10	0.19
CaO	3.68	2.87	3.02	3.94	3.38	4.01	5.67	4.72	4.01	3.93	3.10	1.91	1.86
Na_2O	3.12	4.42	4.35	4.19	4.34	4.24	3.13	1.70	3.40	3.65	3.98	4.20	4.14
K_2O	0.52	0.98	0.64	0.62	0.71	0.55	0.43	0.33	0.18	0.17	0.29	1.06	0.12
P_2O_5	0.03	0.03	0.04	0.05	0.05	0.05	0.06	0.06	0.07	0.07	0.14	0.02	0.06
LOI	1.83	1.71	1.75	1.16	1.32	0.81	1.09	2.45	0.82	0.76	1.72	0.59	0.81
Total	100.19	100.38	99.05	98.97	100.46	100.12	100.29	99.40	100.05	99.99	100.92	100.53	99.22
Sc (ppm)	6.7	7.8	9.0	10.7	11.8	12.5	13.4	13.0	13.4	9.4	7.3	2.9	10.5
V	59	64	55	45	38	55	45	48	62	44	49	10	8
Cr	13	26	2	13	8	7	80	174	12	21	116	18	10
Co	8.6	14.8	13.5	7.9	5.6	7.1	9.3	13.7	6.8	7.3	6.6	2.0	14.3
Ni	15.7	50.2	22.4	78.5	10.4	8.9	8.6	10.5	25.3	5.0	89.1	10.1	14.2
Ga	10.9	11.3	10.7	11.0	10.4	11.2	11.2	8.8	11.6	12.1	15.8	10.0	12.1
Rb	3.8	6.1	3.4	2.4	2.9	2.8	4.1	8.1	2.0	1.5	2.9	20.7	1.6
Sr	160	163	167	170	144	163	159	196	155	155	214	105	91
Y	13.0	13.6	11.3	17.3	18.0	14.2	15.8	17.7	19.4	16.3	13.0	17.9	22.0
Zr	40.3	198.8	46.6	94.9	42.7	51.2	20.7	35.2	80.0	57.8	283.0	61.1	129.8
Nb	1.28	1.05	1.17	0.79	0.69	0.68	0.80	0.80	0.89	1.42	4.13	5.19	0.70
Cs	0.05	0.07	0.10	0.07	0.09	0.06	0.05	0.12	0.04	0.03	0.07	0.13	0.02
Ba	68	69	71	79	74	71	78	67	60	80	198	502	59
La	5.14	2.87	2.97	3.70	2.12	3.28	2.14	3.16	1.50	1.69	21.83	15.45	4.77
Ce	9.58	6.28	6.08	7.89	5.06	6.47	5.00	6.50	4.26	4.56	37.17	27.28	11.27
Pr	1.15	0.84	0.84	1.09	0.77	0.84	0.75	0.94	0.70	0.71	4.23	3.03	1.70
Nd	4.68	3.71	3.91	5.22	3.99	3.89	3.72	4.52	3.51	3.43	14.97	10.13	7.69
Sm	1.37	1.28	1.21	1.59	1.44	1.35	1.50	1.50	1.43	1.33	2.96	2.15	2.31
Eu	0.53	0.53	0.63	0.68	0.60	0.58	0.63	0.65	0.52	0.54	0.82	0.54	0.88
Gd	1.54	1.38	1.33	1.96	1.96	1.69	1.78	1.91	2.00	1.73	2.86	2.27	2.76
Tb	0.28	0.27	0.24	0.38	0.35	0.30	0.33	0.35	0.42	0.35	0.40	0.37	0.51
Dy	1.88	1.88	1.71	2.53	2.67	2.01	2.35	2.45	2.90	2.34	2.12	2.30	3.09
Ho	0.43	0.45	0.38	0.56	0.60	0.46	0.51	0.53	0.60	0.49	0.40	0.50	0.64
Er	1.41	1.38	1.10	1.74	1.81	1.42	1.61	1.68	1.85	1.46	1.18	1.57	1.84
Tm	0.24	0.26	0.19	0.30	0.31	0.24	0.28	0.27	0.31	0.27	0.19	0.30	0.33
Yb	1.58	1.75	1.22	2.04	2.03	1.46	1.76	1.80	2.07	1.68	1.24	2.15	2.13
Lu	0.24	0.30	0.19	0.32	0.32	0.22	0.26	0.27	0.31	0.27	0.21	0.34	0.33
Hf	1.42	5.81	1.48	2.90	1.37	1.65	0.72	1.15	2.08	1.57	6.72	1.43	3.04
Ta	0.11	0.07	0.14	0.10	0.06	0.06	0.07	0.07	0.06	0.10	0.29	0.47	0.04
Pb	1.34	1.39	2.48	1.88	1.41	1.80	1.27	1.17	1.11	0.64	1.82	3.45	1.62
Th	2.17	0.51	0.25	0.26	0.20	0.20	0.23	0.47	0.45	0.33	11.92	4.95	0.61
U	0.30	0.10	0.11	0.09	0.07	0.06	0.05	0.12	0.09	0.09	0.93	0.95	0.13

Fe_2O_3 (t): total iron

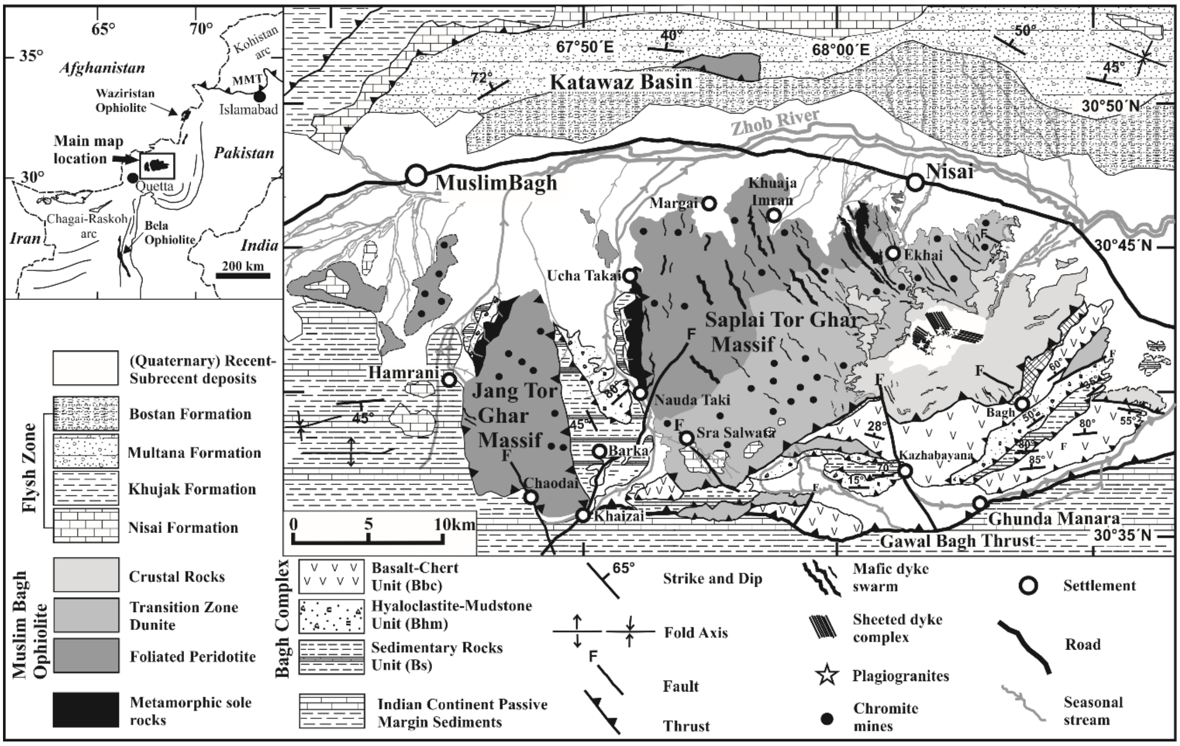
65°
70°
35°
Afghanistan
Kohistan arc
MMT
Waziristan Ophiolite
Islamabad
Main map location
Pakistan
30°
Quetta
Chagai-Raskoh arc
Iran
Bela Ophiolite
India
200 km
67°50´E
68°00´E
Katawaz Basin
30°50´N
Zhob River
MuslimBagh
Nisai
Margai
Khuaja Imran
30°45´N
Ekhai
Ucha Takai
Saplai Tor Ghar Massif
Hamrani
Jang Tor Ghar Massif
Nauda Taki
Sra Salwata
Barka
Chaodai
Khaizai
Kazhabayana
Bagh
Ghunda Manara
Gawal Bagh Thrust
30°35´N
0
5
10km
(Quaternary) Recent-Subrecent deposits
Bostan Formation
Multana Formation
Khujak Formation
Nisai Formation
Flysh Zone
Crustal Rocks
Transition Zone Dunite
Foliated Peridotite
Metamorphic sole rocks
Muslim Bagh Ophiolite
Basalt-Chert Unit (Bbc)
Hyaloclastite-Mudstone Unit (Bhm)
Sedimentary Rocks Unit (Bs)
Bagh Complex
Indian Continent Passive Margin Sediments
Strike and Dip
Fold Axis
Fault
Thrust
Mafic dyke swarm
Sheeted dyke complex
Plagiogranites
Chromite mines
Settlement
Road
Seasonal stream

Figure 1

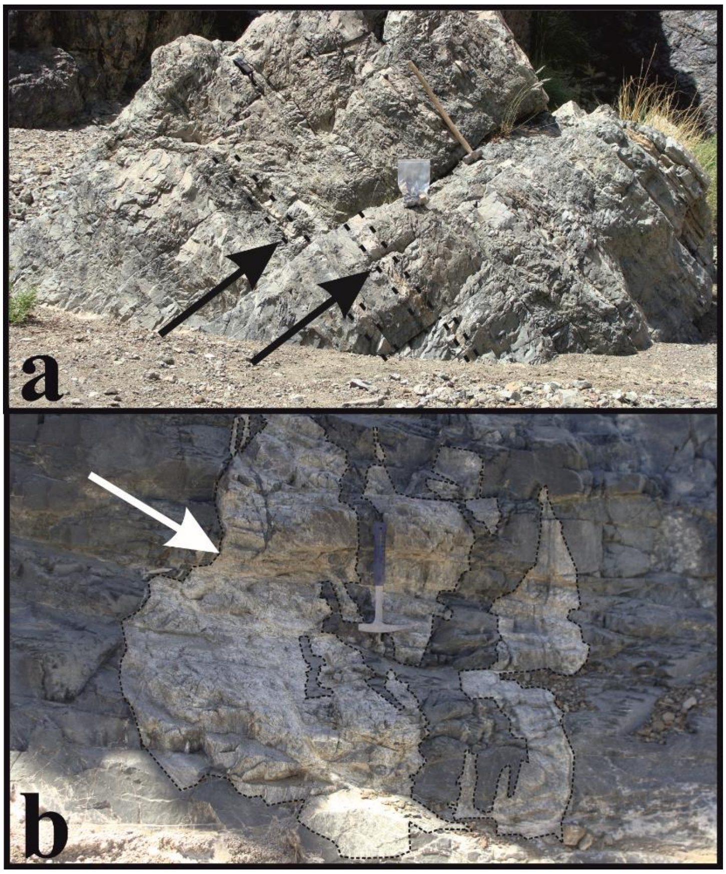

Figure 2

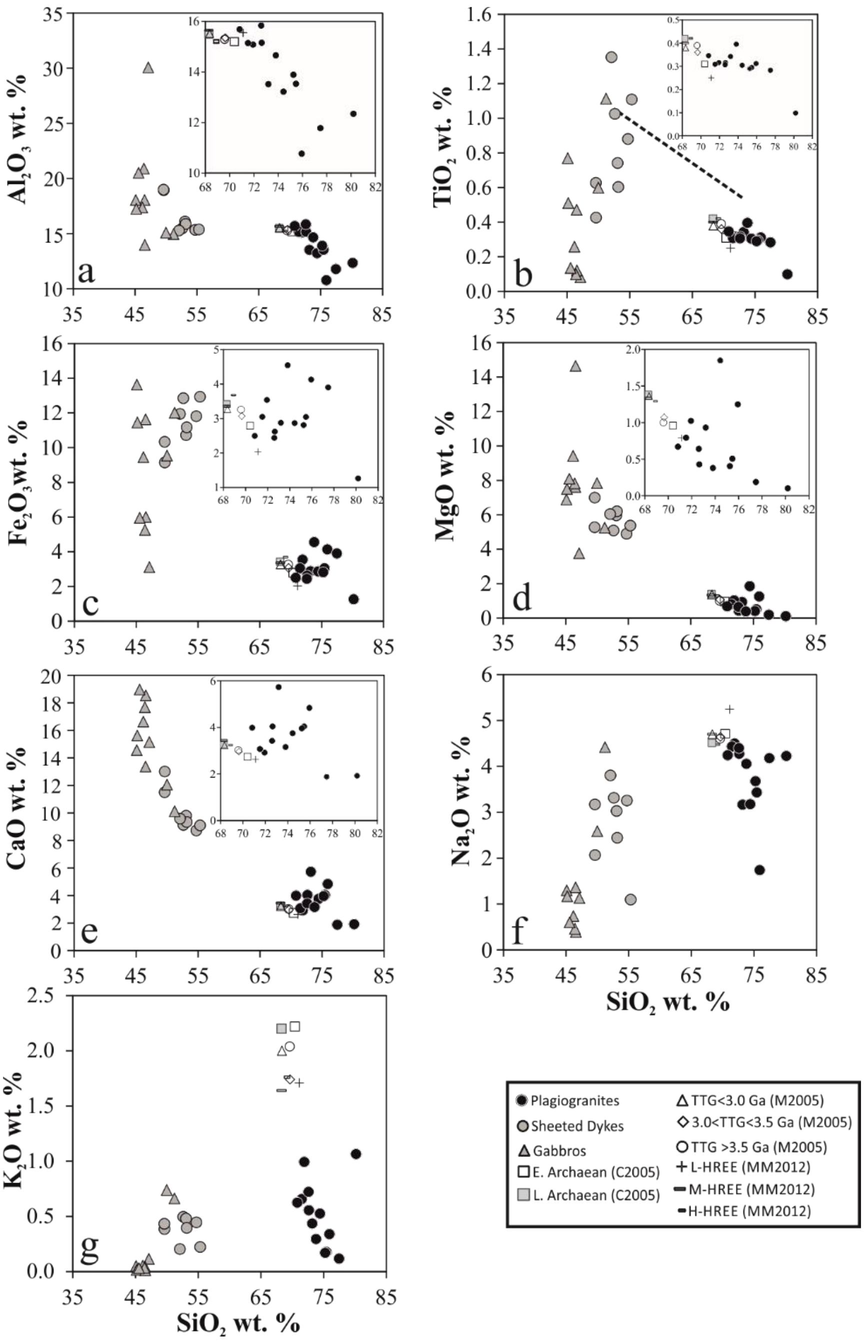
Al_2O_3 wt. %
TiO_2 wt. %
Fe_2O_3 wt. %
MgO wt. %
CaO wt. %
Na_2O wt. %
K_2O wt. %
SiO_2 wt. %
a
b
c
d
e
f
g
Plagiogranites
Sheeted Dykes
Gabbros
E. Archaean (C2005)
L. Archaean (C2005)
TTG<3.0 Ga (M2005)
3.0<TTG<3.5 Ga (M2005)
TTG >3.5 Ga (M2005)
L-HREE (MM2012)
M-HREE (MM2012)
H-HREE (MM2012)

Figure 3

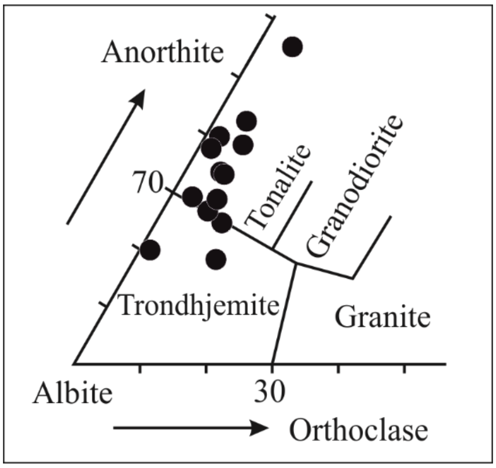
Anorthite
70
Tonalite
Granodiorite
Trondhjemite
Granite
Albite
30
Orthoclase

Figure 4

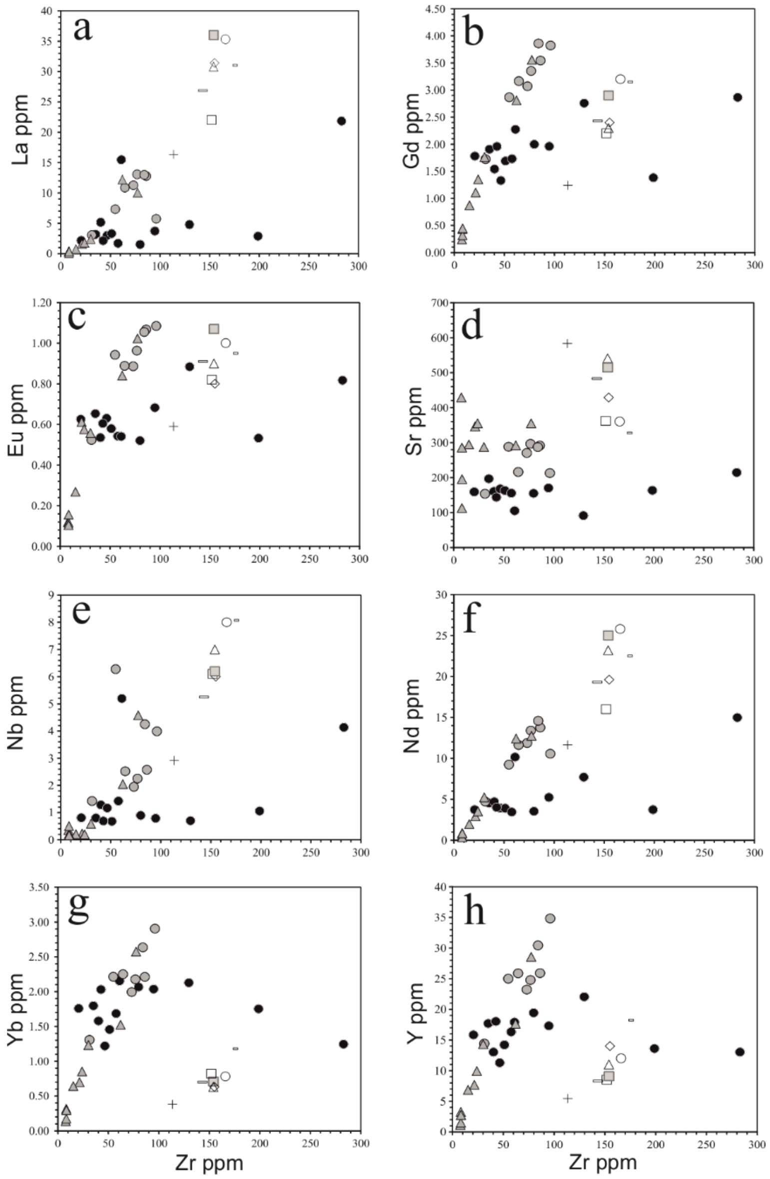
a
La ppm
b
Gd ppm
c
Eu ppm
d
Sr ppm
e
Nb ppm
f
Nd ppm
g
Yb ppm
h
Y ppm
Zr ppm
Zr ppm

Figure 5

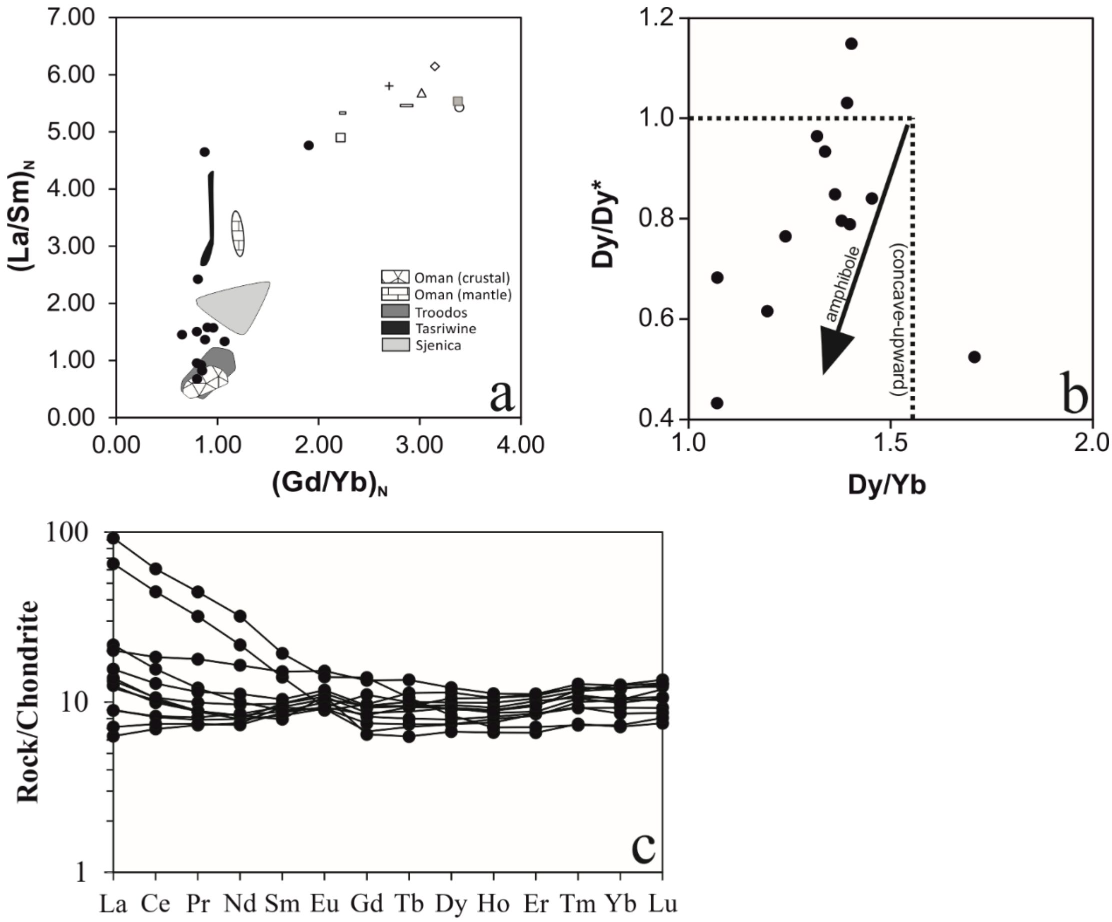
7.00
6.00
5.00
4.00
3.00
2.00
1.00
0.00
(La/Sm)N
0.00
1.00
2.00
3.00
4.00
(Gd/Yb)N
Oman (crustal)
Oman (mantle)
Troodos
Tasriwine
Sjenica
a
1.2
1.0
0.8
0.6
0.4
Dy/Dy*
1.0
1.5
2.0
Dy/Yb
amphibole
(concave-upward)
b
100
10
1
Rock/Chondrite
La
Ce
Pr
Nd
Sm
Eu
Gd
Tb
Dy
Ho
Er
Tm
Yb
Lu
c

Figure 6

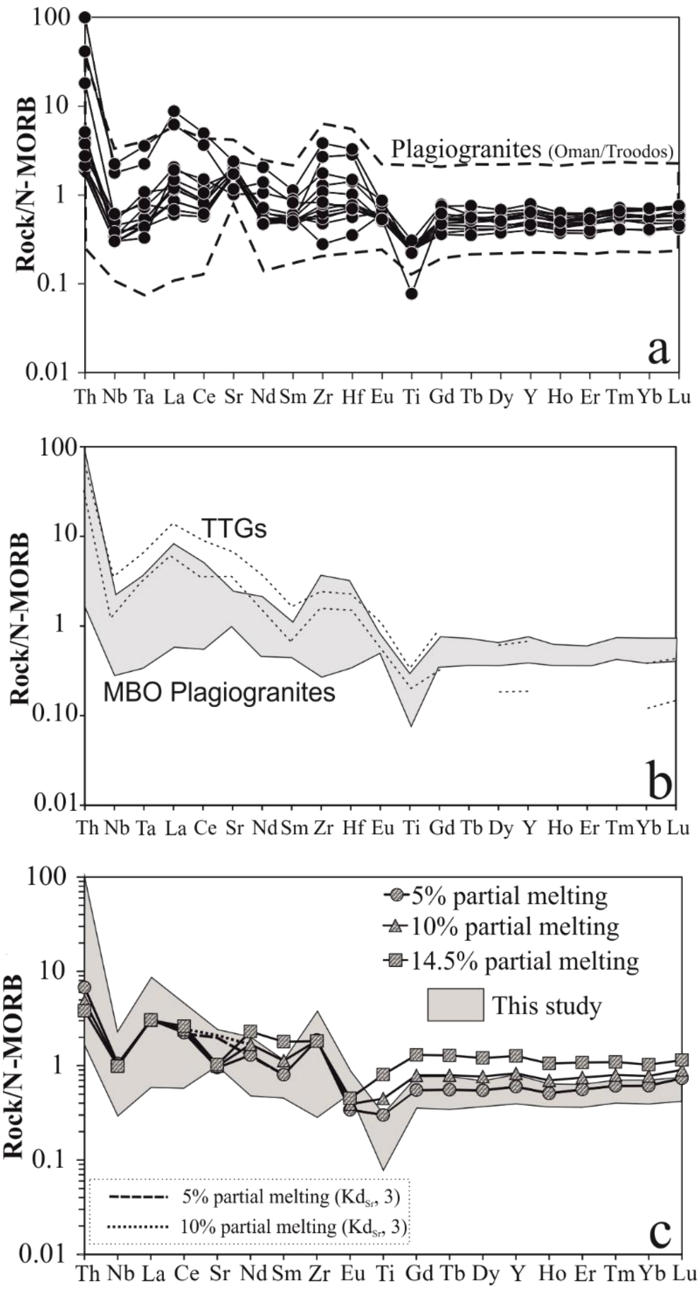
100
10
1
0.1
0.01
Rock/N-MORB
Plagiogranites (Oman/Troodos)
a
Th Nb Ta La Ce Sr Nd Sm Zr Hf Eu Ti Gd Tb Dy Y Ho Er Tm Yb Lu
100
10
1
0.10
0.01
Rock/N-MORB
TTGs
MBO Plagiogranites
b
Th Nb Ta La Ce Sr Nd Sm Zr Hf Eu Ti Gd Tb Dy Y Ho Er Tm Yb Lu
100
10
1
0.1
0.01
Rock/N-MORB
5% partial melting
10% partial melting
14.5% partial melting
This study
5% partial melting (Kd$_{Sr}$, 3)
10% partial melting (Kd$_{Sr}$, 3)
c
Th Nb La Ce Sr Nd Sm Zr Eu Ti Gd Tb Dy Y Ho Er Tm Yb Lu

Figure 7